Bioresource Technology 310 (2020) 123392

Contents lists available at ScienceDirect

Bioresource Technology

journal homepage: www.elsevier.com/locate/biortech

Algal biodiesel production with engineered biochar as a heterogeneous solid acid catalyst

Bunushree Behera, Mari Selvam S, Baishali Dey, Balasubramanian P.*

Agricultural & Environmental Biotechnology Group, Department of Biotechnology & Medical Engineering, National Institute of Technology, Rourkela 769008, India

GRAPHICAL ABSTRACT

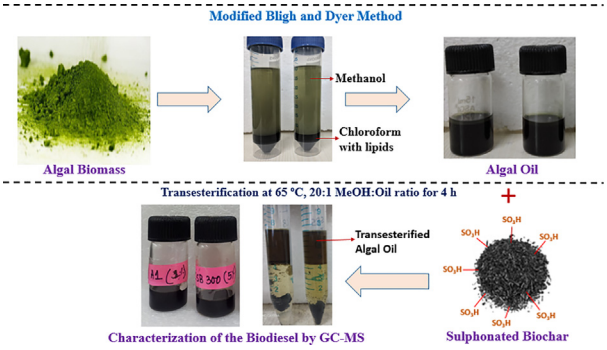

ARTICLE INFO

Keywords:
Engineered biochar
Biodiesel
Microalgae
Surface modification
Transesterification
Pyrolysis

ABSTRACT

This study evaluates the use of engineered biochar as a heterogeneous solid acid catalyst for transesterification of algal oil derived from a native microalgal consortium. Biochar derived from sugarcane bagasse, coconut shell, corncob and peanut shell were evaluated for catalytic activity following surface modification. Peanut shell pyrolyzed at 400 °C with the sulfonic acid density of 0.837 mmol/g having 6.616 m^2/g surface area was selected for efficient catalysis. The efficiency of transesterification was evaluated with 1–7 wt% catalyst loading, methanol: oil ratio of 6:1 to 30:1 at 55–85 °C over 2–8 h. Biodiesel yield of 94.91% was obtained with 5 wt% catalyst loading, MeOH: oil ratio of 20:1 at 65 °C after 4 h. Spectral analysis of algal biodiesel showed the presence of functional groups corresponding to esters. GC–MS analysis revealed the prominent presence of palmitic and oleic acids, further advocating the suitability of the technology for commercial application.

1. Introduction

In today's scenario, the total primary energy consumption is increasing rapidly due to modernization and population explosion. Presently, fossil fuel contributes to about 80% of total world energy demands and the diesel fuel utilization has been predicted to reach 5.7 million litres per day by the year 2035 (Hajjari et al., 2017). Thus, there is global racing for the exploration of potential renewable resources to satisfy the ever-increasing demand for fuel. To meet the growing demands for energy and abate the environmental pollution caused by fossil fuels, there has been a paradigm shift towards renewable biofuels. Biodiesel (mono alkyl fatty acid ester) could act as the potential renewable resource for an alternative of petroleum-based fuels.

The global biodiesel production is predicted to increase by 14% from 2016 to 2020 (OPEC, 2012). Biodiesel, due to its high energy density pertaining to the presence of C14-C20 long carbon chain of

* Corresponding author.
E-mail address: biobala@nitrkl.ac.in (P. Balasubramanian).

https://doi.org/10.1016/j.biortech.2020.123392
Received 31 January 2020; Received in revised form 11 April 2020; Accepted 14 April 2020
Available online 18 April 2020
0960-8524/

triglycerides, is considered to be more favourable for engines (Mohan et al., 2018). Owing to the ethical limitations associated with the first-generation biofuels from edible biomass, there have been increasing interest over the second and third generation biodiesel, especially from microalgae (Behera et al., 2019a). Algal biodiesel has gained significant attention over the years due to their fast growth rate, benign nature to environmental changes and the ability to sequester carbon dioxide (Behera et al., 2019b). Unfortunately, the high processing costs associated during cultivation, harvesting, and further downstream processing and conversion into biodiesel hinders their commercial applications (Rangabhashiyam et al., 2017).

It is essential to reduce the costs associated with the transesterification of algal oil into biodiesel in order to make the algal biofuel economical. Catalysts play an essential role in the transesterification process and can be categorized as homogenous and heterogeneous (Lee et al., 2017). The application of homogenous acid/base catalysts involve the reaction at the interface between alcohol and oil, thus requires extensive stirring (Supraja et al., 2019). Also, the biodiesel formed is often associated with contaminants like glycerol, methanol and residual catalysts, thus requires extensive washing with hot water. Further, the neutralization of the process water before its disposal, adds up to 60% of the downstream processing costs. Owing, to the above-mentioned disadvantages, the use of heterogeneous porous catalysts like metal oxides, zeolites, ion exchange resins that could be recycled has gained attention over years (Lee et al., 2017). However, the acid density of zeolites and metal oxides are extremely low and these substances are reported to be hydrophilic in nature. Ion exchange resins, even though possess higher acid density but are cost-inefficient, thus are unsuitable for large scale application (Sudarsanam et al., 2018). Partial carbonization or pyrolysis of carbonaceous biomass forms a rigid carbon matrix consisting of polycyclic aromatic carbon sheets arranged in three dimensional sp^3 bonded structure where the sulfonic acid ($–SO_3H$) group can easily be functionalized (Chellappan et al., 2018a). Since, carbonization is time-consuming and generates waste by-products, the pyrolyzed biomass are considered as the most efficient and cost-effective carbonaceous material to act as biocatalyst (Anto et al., 2019).

Several studies have reported a significant yield of biodiesel with the use of biochar as a catalyst during the transesterification process (Cheng and Li, 2018; Zhao et al., 2017). Transesterification of waste cooking oil (WCO) with the use of pyrolyzed rice husk biochar lead to 98.17% conversion of free fatty acids, resulting in 87.57% yield of fatty acid methyl esters (FAMEs) (Li et al., 2014). The study by Lee et al. (2017) reported 90% biodiesel yield from WCO with the use of maize residue biochar and 43% biodiesel yield with pine cone biochar, both produced at 450 °C for 3h, thus postulating that the chemical composition of the biomass used for biochar production also influences the activity of catalysts, thereby the transesterification efficiency. Limited studies have been done with the use of biochar as a heterogeneous catalyst for the transesterification of algal oil into biodiesel.

Dong et al. (2015) utilized Douglas Fir based biochar produced at 650 °C for the esterification of algal oil derived from green microalgae *Chlorella sorokiniana* and reported a FAME yield of 99% following a two-step transesterification using calcium oxide-based catalyst. A recent study by Anto et al. (2019) reported a FAME yield of 32.8% from transesterification of algal lipids from *Isochrysis* sp. using rice husk pyrolyzed biomass. The study also reported a 59.06% yield of stearic acid [C18:0] from *P. tricornutum* lipids using rice husk biochar. 69.4% of biodiesel yield was obtained with the utilization of rice hull biochar as a catalyst for the transesterification of *S. obliquus* oil (Ido et al., 2019). Most of the studies done so far with algal oil have utilized only single biochar at specified operational conditions. Since the nature of biochar catalyst depends on the biomass composition and the temperature of the pyrolysis process, it is highly essential to investigate the catalytic potential of different biochar produced at various temperature for the conversion of oil from a specific microalgal consortium.

The present study explores the biodiesel yield via transesterification of algal oil obtained from a native microalgal consortium with acidic biochar catalyst. Physiochemical characterization of four different biochar (i.e.) sugarcane bagasse, corncob, coconut and peanut shell was carried out to explore their catalytic efficiency. The effect of catalyst dose, methanol to oil ratio, temperature and reaction time over biodiesel yield also investigated. The biodiesel obtained was thereby characterized for the presence of fatty acid methyl esters (FAMEs) to evaluate its efficiency as an engine fuel. Such studies would aid in decreasing the downstream processing costs involved with algal biodiesel production process to progress towards a commercial reality.

2. Materials and methods

2.1. Microalgal growth and oil extraction

Microalgal consortium was obtained from the open ponds of National Institute of Technology (NIT) Rourkela and was grown at an ambient temperature of 30 ± 5 °C with the light intensity of 205 μmol photons m^{-2} d^{-1}, in 8:16 light-dark cycle. The operational conditions have already been pre-optimized by the authors and the mixed microalgal consortium predominated with *Chlorella* sp., along with *Scenedesmus* sp., *Synechocystis* sp. and Spi*rulina* sp., as observed through microscopic analysis (Behera et al., 2020). The microalgal biomass was dried and then used for oil extraction. Algal oil was extracted using a modified Bligh and Dyer (1959) method and the yield was quantified based on the equations detailed in Behera et al. (2020).

2.2. Production of biochar via pyrolysis

Four different biomass such as sugarcane bagasse (SB); corncob (CB); coconut shell (CS) and peanut shell (PS) were collected from the areas in and around of NIT Rourkela. The biomass was dried in a hot air oven at 80 °C overnight and the moisture content was found to be below 10%. The biomass was pyrolyzed in a lab-scale electrically heated muffle furnace at three different temperatures of 300 °C, 400 °C, and 600 °C with a heating rate of 10 °C/min. The feedstock was packed inside the covered ceramic crucibles, which was then placed in the closed chamber of the electrically heated lab-scale muffle furnace with no inflow of air/oxygen. The applied heating rate was pre-fixed at 10 °C/min through a digital PID controller system in all cases irrespective of the final pyrolysis temperature to be attained. For further verification, the time required to shoot up for attaining the final set temperature was observed by K-type thermocouple placed inside the furnace. The temperature was allowed to increase and once the desired temperature is reached, it was kept on hold (constant) for the respective time period (1h at 300 °C, and 400 °C and for 30 min at 600 °C). There was no carrier gas involved as the furnace was being operated under self-purging mode, similar to that of the study by Intani et al. (2016). Temperature range from 300 °C to 600 °C, has been meticulously selected based on the previous studies by Zhao et al. (2017); Chellappan et al. (2018a, b) and Cheng and Li (2018) who have postulated that slow pyrolysis at a low heating rate often results in increased yield and better functional properties of biochar. The biochar yield and pH was measured based on the procedure detailed by Chellappan et al. (2018b). The proximate analysis was carried out for each of the sample in accordance with the American Society for Testing and Material (ASTM) D1762-84 protocol.

2.3. Preparation and characterization of acidic biochar

The biochar prepared were subjected to sulfonation by treatment with sulphuric acid. Sulfonation was carried out by subjecting 1 g of biochar with 10 ml of 98% purity sulphuric acid. The mixture was heated at 100 °C for 1h in a hot water bath, followed by shaking at 120 rpm with a temperature of 50 °C for 24h in an orbital shaker. The

Table 1
Physiochemical properties of biochar at different pyrolysis temperature.

Feedstock	Temperature (°C)	pH	Yield (%)	Moisture (%)	Volatile (%)	Ash (%)	Fixed carbon (%)
SB	–	3.7 ± 0.14	–	10.6 ± 0.73	73.89 ± 0.44	3.29 ± 0.34	12.22 ± 0.52
	300	4.2 ± 0.07	56.27 ± 1.20	03.0 ± 0.35	68.45 ± 1.14	3.62 ± 0.30	24.93 ± 2.95
	400	6.5 ± 0.07	50.60 ± 0.03	01.7 ± 0.03	64.44 ± 1.51	5.85 ± 2.54	28.01 ± 3.46
	600	7.6 ± 0.21	18.30 ± 0.03	01.6 ± 2.67	43.18 ± 0.80	6.15 ± 0.70	49.07 ± 2.57
CC	–	6.5 ± 0.14	–	18.5 ± 0.33	73.01 ± 2.37	0.85 ± 0.23	07.64 ± 1.31
	300	7.0 ± 0.07	37.46 ± 0.05	03.1 ± 1.56	71.26 ± 2.94	2.46 ± 0.82	23.18 ± 2.17
	400	7.3 ± 0.07	29.25 ± 0.12	02.4 ± 1.72	67.58 ± 2.57	3.75 ± 1.43	26.27 ± 1.83
	600	8.4 ± 0.14	19.50 ± 0.06	01.6 ± 0.38	47.48 ± 1.08	5.22 ± 1.12	45.70 ± 0.92
CS	–	5.5 ± 0.07	–	10.7 ± 3.06	69.40 ± 1.50	1.57 ± 1.31	18.33 ± 2.54
	300	7.1 ± 0.07	56.35 ± 0.01	03.8 ± 2.05	60.46 ± 1.24	2.69 ± 2.30	33.05 ± 3.11
	400	7.1 ± 0.07	44.87 ± 0.08	04.4 ± 0.14	52.45 ± 2.11	4.32 ± 2.23	38.83 ± 2.06
	600	8.8 ± 0.07	25.80 ± 0.05	02.6 ± 0.48	35.76 ± 0.58	5.63 ± 0.56	56.01 ± 0.63
PS	–	6.7 ± 0.08	–	07.9 ± 0.67	75.06 ± 0.66	2.09 ± 1.90	14.95 ± 1.92
	300	7.3 ± 0.07	55.67 ± 0.08	06.0 ± 1.88	52.39 ± 2.33	3.78 ± 0.62	37.83 ± 2.63
	400	7.9 ± 0.07	52.05 ± 0.03	04.8 ± 2.40	45.36 ± 1.03	4.02 ± 0.69	45.82 ± 1.56
	600	7.9 ± 0.07	25.22 ± 0.04	03.9 ± 0.27	42.32 ± 1.47	5.72 ± 0.52	48.08 ± 1.03

SB: represents sugarcane bagasse biochar; CC: represents corn cob biochar; CS: represents coconut shell biochar; PS: represents peanut shell biochar.

sulfonated solution was cooled to room temperature and then washed with hot deionized water to remove the free sulphate ions. Washing was continued until the pH of filtrate becomes 7. The absence of free sulphate ions was also further confirmed by the lack of formation of precipitate through barium chloride precipitation test.

The functional groups on the surface of sulfonated biochar were detected using Fourier transform infrared spectroscopy (FTIR) by scanning across the wavelength of 400–4000 cm^{-1}. Surface morphology was determined by using the scanning electron microscope (SEM) equipped with energy dispersive X-ray (SEM-EDX) facility. Surface area, pore size and pore volume of the biochar before and after sulfonation was analysed via Brunauer Emmett Teller (BET) surface analyser using N_2 adsorption/desorption process. X-ray diffraction (XRD) was done to detect the crystallographic nature of biochar and sulfonated biochar with 2 theta ranging from 10° to 70°, with a scan rate of 10° per min at a step size of 0.01. Sulfonic acid density was determined using the back titration method as described by Sani et al. (2015). The biochar showing significant acid density with requisite physiochemical properties was further utilized as a catalyst for the transesterification study.

2.4. Transesterification of microalgal oil into biodiesel

Transesterification is often influenced by the amount of catalyst, methanol: oil ratio, temperature and time of reaction. To study the effect of operational parameters over the transesterification process, the reactions were carried out using the acidic biochar catalyst with the amount of catalyst varying from 1% to 7% (wt.) having methanol: oil ratio ranging from of 6:1 to 30:1 at a temperature of 55 °C–85 °C over a period of 2h to 8h. The range of operational conditions for transesterification was selected from the previous literature (Dong et al., 2015; Alaa et al., 2018). The top layer containing biodiesel was separated from the bottom layer containing glycerol. The yield of biodiesel obtained was evaluated based on the study by Alaa et al. (2018). Fatty acid methyl esters (FAMEs) were characterized by Gas Chromatography-Mass Spectrophotometer (Agilent 5977) having a mass-selective detector (MSD) with the programme as given by Sarpal et al. (2016). Biodiesel obtained was also assessed for confirming the presence of functional groups corresponding to esters and other hydrocarbons through FTIR and nuclear magnetic resonance (NMR) analysis as described by Bharti et al. (2014). Physical properties of algal oil and the biodiesel obtained were analysed using the protocols as detailed by Supraja et al. (2019). The cetane number of fuel was estimated based on the physicochemical properties of algal biodiesel using the method as given in Islam et al. (2013) and Sinha et al. (2016).

2.5. Reusability of acidic biochar catalyst

The sulfonated biochar after the first cycle of transesterification was centrifuged and the pellet obtained was washed with acetone to remove any surface contaminants. Pellet obtained was dried in an oven at 60 °C and then used for subsequent cycles of transesterification reaction. The yield of biodiesel obtained for each cycle under the optimized conditions was calculated according to Alaa et al. (2018) for evaluating the stability of sulfonated biochar to act as a catalyst for multiple transesterification process.

3. Results and discussion

3.1. Characterization of biochar

3.1.1. Proximate composition of biomass and characteristic of biochar at different reaction temperature

Biomass was pyrolyzed under slow heating conditions at three different temperatures (300 °C, 400 °C and 600 °C). The effect of pyrolysis temperature and biomass over the biochar yield and the proximate characteristics are presented in Table 1. The quantitative and qualitative yield of biochar products are influenced mainly by the pyrolysis temperature and the kind of feedstocks (Zhao et al., 2017). The abovementioned parameters often differentiate the char formed based on the specific surface area, pore size, pore volume, volatile matter, ash and the fixed carbon content. These parameters have a stronger influence compared to the heating rate and residence time of pyrolysis (Cheng and Li, 2018).

In the present study, with an increase in pyrolytic temperature from 300 °C to 600 °C, there is a sharp decrease in biochar yield for all feedstocks, as most of the lignocellulosic materials have been reported to decompose after 500 °C (Cheng and Li, 2018). Rafiq et al. (2016) also reported a higher biochar yield at lower temperature due to lesser loss of compounds like hydrogen (H_2), methane (CH_4) and carbon monoxide (CO), owing to lower condensation of aliphatic fractions. For, each of the feedstocks, an increase in temperature often resulted in a decrease in volatile fractions similar to the trend as that of the biochar yield, but opposite to that of the trend for fixed carbon. This might be attributed to the fact that the increase in temperature results in thermal cracking of volatile fractions into more of bio-oil and gaseous by-products (Yuan et al., 2015). Further, it was observed that, the increase in temperature often resulted in gradual increase in pH, in case of each of the feedstocks due to the release of alkali salts from organic matter, formation of carbonates and also decrease in –COOH groups (Zhang et al., 2015). Chellappan et al. (2018a) also reported an increase in pH with the increase in pyrolysis temperature from 400 °C to 600 °C due to the decline

in carboxyl groups. An increased ash content was also observed with the increase in temperature from 300 °C to 600 °C owing to the gradual concentration of inorganic residues following massive combustion (Zhao et al., 2017). An increase in ash content of biochar due to the destructive volatilization of lignocellulosic compounds and declining volatile content with the increase in pyrolysis temperature was also reported in the study by Zhang et al. (2015). The carbonization rate, carbon content and the pH was found to increase whereas the yield decreased for corn stover biochar produced at three different temperatures of 300 °C, 400 °C and 500 °C (Rafiq et al., 2016). Chellappan et al. (2018a) also reported that the sawdust biochar produced at 400 °C had higher yield, lower pH and fixed carbon content compared to that produced at 600 °C.

Apart from temperature, the feedstock composition also plays an essential role in determining the yield of products. The chemical composition of feedstocks especially, the lignin and the inorganic constituents like ash content, influences the biochar yield (Cheng and Li, 2018). Since, sugarcane bagasse, coconut and peanut shell have lignin content in the range of 20–40% as available in the literature (Jahirul et al., 2012), thus biochar yield obtained was almost same for sugarcane bagasse (56.27%), coconut shell (56.35%) and peanut shell (55.67%) at 300 °C. However, with corn cob, the maximal biochar yield reported was only 37.46%, probably due to the lower lignin content (15%) in corn cob (Jahirul et al., 2012). Subsequently, higher lignin content in biomass also produces char with a higher amount of fixed carbon (Cheng and Li, 2018). Thus the fixed carbon content was also found to be higher in case of biochar formed from sugarcane bagasse, coconut and peanut shell compared to the corn cob. Also, low ash content of 0.85% for corn cob than sugarcane bagasse, coconut and peanut shell, can be positively correlated to the lower biochar yield in the former biomass compared to the later. Zhao et al. (2017) postulated that the inorganic constituents, especially the alkali and alkaline earth metals present in the biomass often catalyse the pyrolysis reaction resulting in better biochar yield.

The FTIR spectrum of biomass showed the presence of peaks at 1604 cm^{-1} due to the presence of lignin components. However, there was a gradual decline in the peak intensity after pyrolysis especially at 300 °C and 400 °C, showing a reduction in lignocellulosic compounds after pyrolysis. Low-intensity peaks at 1030 cm^{-1} in the pyrolyzed biochar showed relatively less amount of cellulose content compared to the biomass. Cheng and Li (2018) and Zhao et al. (2017) also reported a similar degradation profile for lignocellulosic compounds with the increase in temperature of pyrolysis. Similar observations were earlier reported by Chellappan et al. (2018a, b) for sawdust and cassava peel biochar.

3.1.2. Physiochemical characterization of acidic biochar catalyst

The physical and chemical properties of biochar formed at different temperatures subjected to sulfonation were evaluated for assessing their suitability to act as catalyst for transesterification. The sulfonic acid density of biochar pyrolyzed at different temperature has been represented in Table 2. The highest sulfonic acid density of 0.837 mmol/g was obtained for the peanut shell pyrolyzed at 400 °C (PSS 400). With an increase in pyrolysis temperature, the sulfonic acid density decline was observed irrespective of the feedstock, as complete combustion and aromatization at high temperature, often results in lesser number of acidic functional groups on the surface (Cheng and Li, 2018). Also, high pyrolysis temperature results in increased crosslinking and enhanced degree of polymerization that might not result in formation of polycyclic aromatic sheets, to trap the sulfonic acid sites. With an increase in temperature, the number of polycyclic aromatic carbon sites to be activated on the biochar surface declines, thereby reducing the available acidic sites (Konwar et al., 2019). The stability of sulfonic sites is also dependent on the operational conditions, the morphological and chemical characteristics of the biomass. No sulfonic acid density was detected for sulfonated corn cob and peanut shell biochar produced at 600 °C in the present study. This might also be due to the improper temperature gradient owing to the biochemical characteristic of the biomass, that might not be conducive enough resulting in incomplete formation and crosslinking of polycyclic aromatic sheets to trap sufficient sulfonic acid sites (Qian et al., 2015), which thereby might not be sufficient enough to be detected by acid titration method.

Since PSS 400 exhibited the maximal sulfonic acid density, it was subjected to further examination of chemical characteristics to check its suitability as a catalyst. As evident from Table 3, elemental analysis of PSS 400 showed higher amount of sulphur and oxygen compared to the corresponding biochar due to the process of oxidation and sulfonation. Dong et al. (2015) reported sulfonic acid density of 0.63 mmol/g with 2.02% of sulphur and 33.44% of oxygen content for Douglas fir based acidic biochar. Chellappan et al. (2018a) also reported the presence of 6.62% sulphur and 61.47% oxygen with a sulfonic acid density of 0.8 mmol/g in sawdust biochar formed at 400 °C. The higher amount of sulphur and oxygen obtained is mainly due to the reactions of sulfonation and oxidation during the process of functionalizing the biochar catalyst by acid treatment (Chellappan et al., 2018b).

FTIR spectra were further used to confirm the presence of –COOH and $–SO_3H$ for PSS 400 to act as a solid catalyst. Hydroxyl (–OH) stretching was observed between 2856 and 2919 cm^{-1} in biochar sample after sulfonation. Asymmetric and symmetric stretching of SO_2 was confirmed by the presence of sharp peaks at an intensity of 1031 cm^{-1} and 1170 cm^{-1} compared to the corresponding biochar. Peaks corresponding to –C-O– stretching of carboxyl group was observed at 1210 cm^{-1}. -S=O- stretching was prominently found between 1310 and 1409 cm^{-1}. -S-O- symmetric stretching mode vibration with prominent peaks at 1036 and 1170 cm^{-1} were observed by Chellappan et al. (2018b) for acidic cassava peel biochar. Ido et al. (2019) reported the presence of peaks at 1073 cm^{-1} and 1044 cm^{-1} in the sulfonated moringa leaves based biochar corresponding to the stretching of C-O and S=O respectively. The influence of sulfonic acid pre-treatment over the biochar catalysts was further confirmed by SEM and BET surface area analysis. The SEM images of biochar before and after sulfonation contained heterogeneous surface with several cracks,

Table 2
Sulfonic acid density of biochar before and after sulfonation.

Temperature (°C)	Sulfonic density of biochar (mmol/g)							
	SB	SBS	CC	CCS	CS	CSS	PS	PSS
300	0.04 ± 0.01	0.29 ± 0.03	ND	0.35 ± 0.26	ND	0.45 ± 0.02	ND	0.011 ± 0.003
400	ND	0.15 ± 0.01	ND	0.31 ± 0.02	ND	0.19 ± 0.01	ND	0.837 ± 0.120
600	ND	0.04 ± 0.04	ND	ND	ND	0.12 ± 0.01	ND	ND

*ND represents not detected.
SB: represents sugarcane bagasse biochar; SBS represents sugarcane bagasse sulfonated biochar.
CC: represents corn cob biochar; CCS represents corn cob sulfonated biochar.
CS: represents coconut shell biochar; CSS represents coconut shell sulfonated biochar.
PS: represents peanut shell biochar; PSS represents peanut shell sulfonated biochar.

Table 3
Elemental analysis and physicochemical characteristics of the sulfonated biochar catalyst.

Biochar	Elemental composition (%)					Surface area (m^2/g)	Pore size (nm)	Pore volume (cc/g)	Sulfonic acid density (mmol/g)
	C	H	N	S	O				
PS 400	47.16	0.57	1.47	4.80	46.00	1.185	4.47	0.020	ND
PSS 400	16.09	0.48	0.54	9.02	73.87	6.616	2.98	0.059	0.837

fissures, crevices with rough and irregular edges. It can be observed that the particle size was much more reduced following sulfonation due to the breakdown of organic matter by the action of acid (Fadhil et al., 2016). The sulfonated peanut shell biochar showed higher surface area and pore volume compared to the untreated biochar, thus providing enough active sites for the incorporation of sulfonic acid groups as shown in Table 3. Similar results were also reported by Dong et al. (2015) and Bhatia et al. (2020) for sulfonated Douglas fir and waste cork biochar respectively.

XRD analysis of the peanut shell biochar showed a broad peak corresponding to the diffraction of carbon (C004) indicating the presence of amorphous carbon structure with randomly oriented sheets. Narrowing of peak showed more ordered open graphite-like carbon lattice structure, which further specifies it as a stable carbonaceous material (Bhatia et al., 2020). PSS 400 also showed the presence of carbon sulphide (–CS) functional groups which were absent in the untreated sample. A decrease in peak intensities and more disordered structure after sulfonation might be attributed to the attachment of $–SO_3H$ groups to the sp^2 carbon network (Fadhil et al., 2016). Chellappan et al. (2018a, b) also reported disorientation of carbon lattice upon sulfonation in sawdust and cassava peel biochar pyrolyzed at 400 °C.

3.2. Transesterification of algal oil

3.2.1. Effect of catalyst dose on biodiesel yield

The influence of catalyst over the biodiesel yield was evaluated by varying the dose from 1 to 7 wt%, keeping the methanol: oil ratio of 9:1 at 65 °C after 4h of transesterification. At low catalyst dose of 1 wt% and 3 wt%, the biodiesel yield of 55.04 ± 0.036% and 85.03 ± 0.005% respectively was obtained. Biodiesel yield of 91.04 ± 0.001% was achieved with a catalyst dose of 5 wt%, which slightly declined to 89.27 ± 0.006% with further increase in catalyst dose to 7 wt%. Surface area available for the reaction increases with an increase in the amount of catalyst, therefore the efficiency of transesterification process increases (Farooq et al., 2015). However, the reaction reaches a saturation point after a certain period of time, due to the unavailability of reactant (MeOH), thus beyond the threshold value any further increase in catalyst concentration has no significant effect over the yield of products (Supraja et al., 2019). Similar to the present study, Dong et al. (2015) also reported maximum yield of algal biodiesel at acidic biochar based catalyst amount of 5 wt%, which further declined with the increase in catalyst dose. Similar results were also obtained in the study by Anto et al. (2019) and Bhatia et al. (2020). Increase in catalyst dose beyond the optimum amount often results in an increase in mass transfer resistance due to an increase in viscosity of the reaction mixture, thereby declining the transesterification efficiency (Dong et al., 2015).

3.2.2. Effect of methanol: Oil ratio on biodiesel yield

Methanol: oil (MeOH: oil) ratio plays an essential role in the progress of the transesterification reaction. The influence of methanol: oil ratio varying from 6:1 to 30:1 over the biodiesel yield was observed while keeping the 5 wt% catalyst amount at 65 °C for 4h. The biodiesel yield increased gradually from 38.24 ± 0.004% to 91.04 ± 0.001% and then to 94.91 ± 0.006% with an increase in MeOH: oil ratio from 6:1 to 9:1 and then to 20:1 respectively. Obadiah et al. (2012) reported that the increase in methanol: oil ratio often results in an increase in biodiesel yield due to the progress of reaction in the forward direction. Dong et al. (2015) experimented with methanol: oil ratio of 5:1, 10:1 and 20:1 and reported the maximal FAME yield at methanol: oil ratio of 20:1 as more triglycerides dissolved in methanol at higher concentration. It was observed that with further increase in MeOH: oil ratio beyond the threshold limit of 20:1 to 30:1, the biodiesel yield declined to 79.82 ± 0.003%. Bhatia et al. (2020) also reported that an increase in alcohol: oil ratio beyond 25:1 often results in inhibition of transesterification of waste cooking oil (WCO) as the glycerol formed often dissolve in excess of methanol, thereby influencing the forward reaction. The optimal ratio of alcohol: oil depends on the nature of oil as well as other operating parameters of transesterification which influences the miscibility of oil (Dong et al., 2013).

3.2.3. Effect of reaction temperature on biodiesel yield

Temperature plays a significant role in the progress of transesterification as it influences the kinetics and equilibrium of the process (Alaa et al., 2018). The effect of variation in temperature (55 °C–85 °C over the transesterification process with 5 wt% PSS 400 at MeOH: oil ratio of 20:1 after 4h was evaluated. With an increase in temperature from 55 °C to 65 °C, a gradual increase in the biodiesel yield was observed from 31.29 ± 0.033% to 94.91 ± 0.006%. Zeng et al. (2014) and Dong et al. (2015) also reported an increase in biodiesel yield with the increase in temperature due to increased miscibility of triglycerides in methanol. However, with further increase beyond 65 °C to 75 °C and then to 85 °C a decline in biodiesel yield to 68.72 ± 0.069% and 29.21 ± 0.041% was observed respectively. High temperature beyond the threshold range often favours saponification, thereby decreasing the methyl esters content (Supraja et al., 2019). The optimal temperature for transesterification also depends on the nature of oil as well as the solvent used (Alaa et al., 2018).

3.2.4. Effect of reaction time on biodiesel yield

The effect of reaction time from 2 to 8h on biodiesel yield keeping MeOH: oil ratio at 20:1 with 5 wt% of catalyst amount at 65 °C was studied, as the residence time influences the transesterification efficiency. It was seen that with an increase in time from 2h to 4h, the yield of biodiesel was found to increase from 35.83 ± 0.021% to 94.91 ± 0.006%. This might be attributed to the fact that the reactants require a certain minimum time period in order to react and form the requisite products (Wang et al., 2017). However, with further increase in exposure time to 6h and 8h, the yield of biodiesel was found to decline to 85.86 ± 0.198% and 82.70 ± 0.264% respectively. The decline in yield might be attributed to the formation of more of mono and diglycerides (Supraja et al., 2019). Zeng et al. (2014) also reported a decline in the conversion of cotton seed oil to biodiesel with peanut shell biochar as a catalyst with an increase in residence time of transesterification from 0.5h to 2h. Nuradila et al. (2017) reported 90% biodiesel yield with methanol: oil ratio of 9:1, after 2h of transesterification for canola oil with the use of acidic palm kernel shell biochar, which was found to decline further with prolonged time. Thus, depending on the characteristics of oil and the solvent used for transesterification, there exists an optimum reaction time which influences the yield (Supraja et al., 2019).

3.3. Characterization of algal biodiesel

3.3.1. Analysis of hydrocarbon and FAMEs in biodiesel

The algal biodiesel obtained with 5 wt% loading of PSS 400 at 65 °C with 20:1 MeOH: oil ratio after 4h was analysed for the presence of functional groups corresponding to hydrocarbons and FAMEs via FTIR and NMR analysis. Prominent peaks corresponding to –C–H– stretch of triacylglycerol were evident between 2500 and 3000 cm^{-1}. –C = O– stretching was seen in the region of 2000–2500 cm^{-1}. –C-O-C– and –CH bending were observed in the regions of 900–1400 cm^{-1}. Peaks at 1733 cm^{-1} correspond to –C = O– group present in esters. The presence of a band at 1165 cm^{-1} signifies the existence of methyl group near the carbonyl group. The FTIR spectra clearly revealed the conversion of algal lipids into biodiesel. Similar spectra with the presence of infrared peaks corresponding to the carbonyl group and esters were also reported for biodiesel by Bharti et al. (2014). Characteristic peaks corresponding to the presence of methyl esters were also obtained in the algal biodiesel by Rahman and Nahar (2016).

^{1}H and ^{13}C NMR spectra of algal biodiesel revealed the presence of functional groups corresponding to FAMEs. The proton resonance and peaks were identified based on the study by Bharti et al. (2014). The peaks corresponding between 7.285 ppm and 8.111 ppm can be attributed to olefinic protons. The presence of acyl groups in triacylglycerol can be detected by peaks resonating between 2.30 ppm and 1.60 ppm. Methylene group of ester was evident from the peak at 2.31 ppm. The methyl group (–CH_2–) backbone was visibly present due to the peak between 1.22 ppm and 1.90 ppm. C1 and C3 methylene group protons of glycerol in triacylglycerol resonate at 4.03 ppm and 4.34 ppm respectively, thus suggesting the presence of triacylglycerol. ^{13}C peaks located between 14.02 ppm and 41.34 ppm, and 76.67 ppm and 77.31 ppm were due to the presence of carbons in triacylglycerol of algal biodiesel. Resonance of peaks at 206.74 ppm was attributed to the glycerol backbone and unsaturated carbon respectively. Sarpal et al. (2016) also reported similar spectral peaks for the FAMEs obtained from *S. ecornis* and *C. vulgaris*.

The GC–MS analysis of the biodiesel obtained has been summarized in Table 4. The biodiesel obtained were mainly consisted of FAMEs from C16 and C18 groups. 59.73% FAME was reported in the biodiesel obtained from algal oil following transesterification with 5% (wt.) peanut shell acidic biochar as catalyst with 20:1 MeOH: oil ratio at 65 °C after 4h. 16.83% of oleic acid (C18:1) followed by 12.15% of palmitic acid (C16:0) and 9.45% of linoleic acid (C18:2) was present in the algal biodiesel. The presence of 15.45% of saturated fatty acids in the algal biodiesel indicated it to be suitable as fuel with probably high oxidative stability and cetane number (Mohan et al., 2018). 32.8% of FAMEs has been reported in the biodiesel obtained by transesterification of lipids from *Isochrysis* sp. by acidic rice husk biochar (Anto et al., 2019). Presence of significant amount of specific FAMEs comprising of palmitic acid (C16:0) and oleic acid (C18:1) revealed its potential suitability for engines (Bharti et al., 2014). Similar to the present study, Dong et al. (2015) have also reported that the biodiesel obtained from acidic biochar based transesterification of *C. sorokiniana* had methyl esters with mostly 16 and 18 carbon chains indicating it to be appropriate for fuel applications.

3.3.2. Physiochemical properties of biodiesel

The biodiesel produced must be properly quantified and analysed to meet the standard norms of ASTM and European agencies to be technically and commercially feasible. In the present study, 10 g of dried microalgal biomass produced 2.7 g of algal oil. Further, 10 g of algal oil in the present study was transesterified in the presence of 5% (wt.) of sulfonated peanut shell biochar catalyst under optimized conditions, producing 9.4 g of algal biodiesel, thus from 10 g algal biomass, 2.4 g of algal biodiesel was obtained. The results are in accordance with the study by Kais et al. (2011) that projected 2 g of biodiesel obtained from 10 g of dried biomass of *Chlorella* sp. Thus, based on the previous literature, the process was found to be technically feasible based on the quantity of biodiesel produced.

Table 4
GC–MS analysis of compounds present in algal biodiesel.

PeakNo.	Retention time (min)	Compound Name	Area (%)
1	5.064	2 Amino 6 methyl benzoic acid	0.39
2	6.324	Propanoic acid octyl ester	0.25
3	7.129	Pentadecyl ester	0.09
4	8.322	Cyclo pentyl ester	0.05
5	9.469	Propenoic acid	0.18
6	13.978	Pentadecyl Propyl ester	0.63
7	14.279	Cis-vaccenic acid	0.97
8	15.327	6 Octadecanoic acid	0.20
9	16.691	Pentadecanoic acid methyl ester	0.43
10	16.733	Pentafluoro propionic acid tetra decyl ester	0.76
11	17.086	Pentadecanoic acid methyl ester	0.12
12	18.121	Hexadecanoic acid methyl ester (Palmitic acid)	12.15
13	18.772	Pentadecyl ester	1.12
14	19.260	9,12 Octadecanoic acid (Linoleic acid)	9.45
15	19.343	Cis-13-Octadecanoic acid	5.50
16	19.493	Valeric acid 4 pentadecyl ester	1.14
17	19.836	9 Octadecanoic acid methyl ester (Oleic acid)	16.83
18	20.054	Stearic acid	2.92
19	20.334	Trans 2 octadecanoic acid	0.87
20	20.505	7,12 octadecanoic acid	1.40
21	20.687	Penta fluoro propionic acid	2.89
22	21.190	Trans 13 octadecanoic acid	1.39

*FAME constitutes 59.73%, while 40.27% consisted of alkanes, aldehydes and alcohols.

Table 5 shows the physicochemical properties of algal oil as well as the biodiesel obtained after transesterification with biochar based acidic catalyst. It was found that the acid value and free fatty acids (FFA) of algal biodiesel were less compared to the algal oil, thus indicating the conversion of FFA into triacylglycerol. Saponification and iodine value were also found to decline. Higher iodine number obtained in the present study relates to a higher degree of unsaturation, therefore beneficial cold filter plugging point and better flow properties especially at low temperature (Islam et al., 2013). The density of algal biodiesel was found to be 0.87 g/cc. Biodiesel from *C. sorokiniana* obtained via transesterification with acidic biochar as catalyst showed kinematic viscosity of 4.39 mm^2 /s and density of 0.87 g/cc (Dong et al., 2015).

The cetane number of the algal biodiesel in the present study was estimated to be 68.55. Cetane number is the most efficient indicator that measures the ignition quality of the biofuel. Higher cetane number is related to shorter ignition delay, resulting in quicker ignition and better fuel combustion (Sinha et al., 2016). Increase in cetane number raises the temperature of combustion chamber, which further enhances the oxidation rate, thereby reducing the amount of unburnt hydrocarbons due to less non-ignited fuel built in the combustion chamber. Thus, the fuel efficiency increases, less particulate matter is being built up, thereby declining the harmful gaseous emissions (Sinha et al., 2016). Similar to the present study, Singh et al. (2017) have reported a cetane number of 64 for algal biodiesel obtained from *Neochlorosis oleoabundans* using conventional transesterification. Islam et al. (2013) reported cetane number of algal biodiesel for 21 different microalgal species ranging from 28.6 to 63.3. Cetane number for microalgal biodiesel ranging from 46.77 to 69.62 was reported by Sinha et al. (2016) for 11 isolates of microalgae. According, to ASTM D6751-02 and EN14214, the cetane number of fuel should range in between 47 and 51, whereas the iodine value can be set as max. of 120 g I_2/ 100g fat. Higher cetane number-based biodiesel can be blended to provide better fuel efficiency (Islam et al., 2013). Since, Indian standards for biodiesel

Table 5
Physiochemical properties of algal biodiesel obtained using PSS biochar as a heterogeneous solid acid catalyst.

Parameters	Algal Oil	Biodiesel	ASTM Standard (D6751-02)	European Standard (EN 14214)
Density (g/cc)	0.89	0.87	0.86–0.90	0.86–0.90
Saponification value (mg KOH/g)	175.55	110.2	–	–
Acid value (mg KOH/g)	2.51	1.09	0.50	0.50
Iodine number (g I_2/100 g fat)	191.21	121.20	–	120
Ester Value (mg KOH/g)	173.04	109.11	–	–
FFA content (%)	1.26	0.54	1–2	–

recommends 20% blending for biodiesel, the algal biodiesel obtained can be blended in higher concentrations with the conventional diesel (cetane number 48–52) to be used in diesel-powered engines. Similar properties of algal diesel were also reported by Suganya et al. (2013) and Rahman and Nahar (2016) for the biodiesel obtained from *E. compressa* and *Spirulina maxima* respectively. Karmakar et al. (2018) also showed that the properties of biodiesel obtained from a native algal consortium were found to be suitable for application in diesel engine.

3.4. Reusability of catalyst

To reduce the costs involved with the preparation of heterogeneous catalysts it is essential to assess the reusability of catalysts following the series of transesterification. The yield of biodiesel was evaluated taking 5 wt% of sulfonated peanut shell biochar with 20:1 MeOH: oil ratio at 65 °C after 4h until 5 cycles of transesterification. Yield was found to gradually decline from 94.91 ± 0.006%, to 91.56 ± 0.004%, 87.16 ± 0.005%, 83.51 ± 0.029% after 2nd, 3rd and 4th cycle of transesterification respectively. A further decline in yield to 79.85 ± 0.049% was observed after the 5th cycle of transesterification. The decrease in yield might be attributed to the leaching of sulfonic acid sites after several cycles of reaction (Chellappan et al., 2018a). Dong et al. (2015) also reported a decrease in fatty acid conversion from 98% to 83% for *C. sorokiniana* biodiesel after 3 cycles of transesterification. Chellappan et al. (2018b) with the use of acidic cassava peel biochar as a catalyst also reported a decline to 87% from 96% biodiesel yield after 4 cycles. Nevertheless, the durability of the biochar catalyst is evident from its stability and biodiesel yield obtained after subsequent cycles.

Also, it is noteworthy to mention that the acidified biochar even after transesterification still possesses the properties of surface complexation and precipitation due to the presence of desired functional groups, and it could be utilized for environmental remediation. Uchimiya et al. (2012) reported that recalcitrant biochar rich in carbonyl group could be utilized as long term stabilizing agent for adsorbing heavy metals from water and soil samples. Hadjittofi et al. (2014) reported that the presence of carboxyl group, hydrophilicity of biochar after surface activation resulted in increased moiety towards Cu (II) adsorption from water. Wang et al. (2017) reported that the engineered biochar through chemical activation could be utilized as an adsorbent for CO_2 and other noxious gases. Thus, the exhausted biochar still retaining the high surface area, porosity and functional groups could be used as such/remodified for a multitude of applications in interdisciplinary fields ensuring the process sustainability.

4. Conclusion

Acidified peanut shell biochar acts as an efficient catalyst for the transesterification of algal oil in a renewable manner. Nature of biomass and pyrolysis temperature influenced the catalytic efficiency of biochar. 94.91% biodiesel yield with 59.73% FAMEs was obtained at optimum conditions of 5 wt% catalyst loading on 65 °C for 20:1 MeOH: oil ratio after 4h. Presence of significant amount of C18:1 and C16:0 FAMEs in the algal biodiesel revealed its potential for engine applications. Acidified biochar catalyst could reduce the downstream processing costs as well as reduce the environmental impacts associated with the corrosive chemicals.

5. Authors' contribution

PB has initiated the concept of the project. BB, MS and BD have done the experiments and collected the data for interpretation. BB have drafted the manuscript. PB has reviewed and finalized the manuscript. All authors read and approved the final manuscript for peer review and possible publication.

Declaration of Competing Interest

The authors declare that they have no known competing financial interests or personal relationships that could have appeared to influence the work reported in this paper.

Acknowledgement

The authors thank the Department of Biotechnology and Medical Engineering of National Institute of Technology Rourkela for providing the research facility. The authors greatly acknowledge the Ministry of Human Resources Development (MHRD) of Government of India (GoI) for sponsoring the PhD programme of the first author. The authors thank the Science and Engineering Research Board (SERB), Department of Science and Technology (DST, GoI) for the research grant [File No: ECR/2017/003397].

Appendix A. Supplementary data

Supplementary data to this article can be found online at https://doi.org/10.1016/j.biortech.2020.123392.

References

Alaa, H., Jamil, F., Al-Haj, L., Myint, M.T.Z., Mahmoud, E., Ahmad, M.N., Rafiq, S., 2018. Biodiesel production over a catalyst prepared from biomass-derived waste date pits. Biotech Rep. 20, e00284.
Anto, S., Karpagam, R., Renukadevi, P., Jawaharraj, K., Varalakshmi, P., 2019. Biomass enhancement and bioconversion of brown marine microalgal lipid using heterogeneous catalysts mediated transesterification from biowaste derived biochar and bionanoparticle. Fuel. 255, 115789.
Behera, B., Acharya, A., Gargey, I.A., Aly, N., Balasubramanian, P., 2019a. Bioprocess engineering principles of microalgal cultivation for sustainable biofuel production. Bioresour Technol Rep. 5, 297–316.
Behera, B., Aly, N., Balasubramanian, P., 2019b. Biophysical model and techno-economic assessment of carbon sequestration by microalgal ponds in Indian coal based power plants. J. Clean Prod. 221, 587–597.
Behera, B., Patra, S., Balasubramanian, P., 2020. Biological nutrient recovery from human urine by enriching mixed microalgal consortium for biodiesel production. J. Environ Manag. 260, 1–13.
Bharti, R.K., Srivastava, S., Thakur, I.S., 2014. Production and characterization of biodiesel from carbon dioxide concentrating chemolithotrophic bacteria, *Serratia sp.* ISTD04. Bioresour Technol. 153, 189–197.
Bhatia, S.K., Gurav, R., Choi, T.R., Kim, H.J., Yang, S.Y., Song, H.S., Kim, S.H., 2020. Conversion of waste cooking oil into biodiesel using heterogeneous catalyst derived from cork biochar. Bioresour Technol. 122872.
Bligh, E.G., Dyer, W.J., 1959. A rapid method of total lipid extraction and purification. Can. J. Biochem. Physiol. 37, 911–917.
Chellappan, S., Nair, V., Sajith, V., Aparna, K., 2018a. Synthesis, optimization and

characterization of biochar based catalyst from sawdust for simultaneous esterification and transesterification. J *Chinese journal Chem. Eng.* 26 (12), 2654–2663.
Chellappan, S., Nair, V., V, S., K, A.,, 2018b. Experimental validation of biochar based green Bronsted acid catalysts for simultaneous esterification and transesterification in biodiesel production. Bioresour Technol Rep. 2, 38–44.
Cheng, F., Li, X., 2018. Preparation and application of biochar-based catalysts for biofuel production. Catalysts. 8 (9), 346–385.
Dong, T., Gao, D., Miao, C., Yu, X., Degan, C., Garcia-Pérez, M., Chen, S., 2015. Two-step microalgal biodiesel production using acidic catalyst generated from pyrolysis-derived bio-char. Energy Convers. Manag. 105, 1389–1396.
Dong, T., Wang, J., Miao, C., Zheng, Y., Chen, S., 2013. Two-step in situ biodiesel production from microalgae with high free fatty acid content. Bioresour. Technol. 136, 8–15.
Fadhil, A.B., Aziz, A.M., Al-Tamer, M.H., 2016. Biodiesel production from *Silybum marianum* L. seed oil with high FFA content using sulfonated carbon catalyst for esterification and base catalyst for transesterification. Energy Convers. Manag. 108, 255–265.
Farooq, M., Ramli, A., Naeem, A., 2015. Biodiesel production from low FFA waste cooking oil using heterogeneous catalyst derived from chicken bones. Renew. Energy. 76, 362–368.
Hadjittofi, L., Prodromou, M., Pashalidis, I., 2014. Activated biochar derived from cactus fibres–preparation, characterization and application on Cu (II) removal from aqueous solutions. Bioresour. Technol. 159, 460–464.
Hajjari, M., Tabatabaei, M., Aghbashlo, M., Ghanavati, H., 2017. A review on the prospects of sustainable biodiesel production: A global scenario with an emphasis on waste-oil biodiesel utilization. Renew. Sust. Energ. Rev. 72, 445–464.
Ido, A.L., de Luna, M.D.G., Ong, D.C., Capareda, S.C., 2019. Upgrading of *Scenedesmus obliquus* oil to high-quality liquid-phase biofuel by nickel-impregnated biochar catalyst. J. Clean Prod. 209, 1052–1060.
Intani, K., Latif, S., Kabir, A.R., Müller, J., 2016. Effect of self-purging pyrolysis on yield of biochar from maize cobs, husks and leaves. Bioresour. Technol. 218, 541–551.
Islam, M.A., Magnusson, M., Brown, R.J., Ayoko, G.A., Nabi, M., Heimann, K., 2013. Microalgal species selection for biodiesel production based on fuel properties derived from fatty acid profiles. Energies. 6 (11), 5676–5702.
Jahirul, M.I., Rasul, M.G., Chowdhury, A.A., Ashwath, N., 2012. Biofuels production through biomass pyrolysis—a technological review. Energies. 5 (12), 4952–5001.
Kais, M.I., Chowdhury, F.I., & Shahriar, K.F., 2011. Biodiesel from Microalgae as a solution of third world energy crisis. In: World Renewable Energy Congress-Sweden; 8-13 May; 2011; Linköping; Sweden (No. 057, pp. 192-199). Linköping University Electronic Press.
Karmakar, R., Kundu, K., Rajor, A., 2018. Fuel properties and emission characteristics of biodiesel produced from unused algae grown in India. Petrol Sci. 15 (2), 385–395.
Konwar, L.J., Mäki-Arvela, P., Mikkola, J.P., 2019. SO3H-Containing Functional Carbon Materials: Synthesis, Structure, and Acid Catalysis. Chem Rev. 119 (22), 11576–11630.
Lee, J., Jung, J.M., Oh, J.I., Ok, Y.S., Lee, S.R., Kwon, E.E., 2017. Evaluating the effectiveness of various biochars as porous media for biodiesel synthesis via pseudo-catalytic transesterification. Bioresour Technol. 231, 59–64.
Li, M., Zheng, Y., Chen, Y., Zhu, X., 2014. Biodiesel production from waste cooking oil using a heterogeneous catalyst from pyrolyzed rice husk. Bioresour Technol. 154, 345–348.
Mohan, S.V., Pandey, A., Varjani, S. (Eds.), 2018. Biomass, Biofuels, Biochemicals: Microbial Electrochemical Technology: Sustainable Platform for Fuels. Elsevier, Chemicals and Remediation.
Nuradila, D., Ghani, W.A.W.A.K., Alias, A.B., 2017. Palm kernel shell-derived biochar and catalyst for biodiesel production. Malaysian J. Anal. Sci. 21 (1), 197–203.
Obadiah, A., Swaroopa, G.A., Kumar, S.V., Jeganathan, K.R., Ramasubbu, A., 2012. Biodiesel production from palm oil using calcined waste animal bone as catalyst. Bioresour Technol. 116, 512–516.
OPEC-2012 world oil outlook_. 2013. [accessed on 20th November 2016, Available at: ⟨http://www.opec.org/opec_web/static_files_project/media/downloads/publications/WOO_2013.pdf⟩].
Qian, K., Kumar, A., Zhang, H., Bellmer, D., Huhnke, R., 2015. Recent advances in utilization of biochar. Renew. Sust. Energ. Rev. 42, 1055–1064.
Rafiq, M.K., Bachmann, R.T., Rafiq, M.T., Shang, Z., Joseph, S., Long, R., 2016. Influence of pyrolysis temperature on physico-chemical properties of corn stover (*Zea mays* L.) biochar and feasibility for carbon capture and energy balance. PloS One. 11 (6).
Rahman, M.A., Nahar, K., 2016. Production and characterization of algal biodiesel from Spirulina maxima. J. Global Res. Eng.
Rangabhashiyam, S., Behera, B., Aly, N., Balasubramanian, P., 2017. Biodiesel from microalgae as a promising strategy for renewable bioenergy production-A review. J Environ Biotech Res. 6, 260–269.
Sani, Y.M., Raji-Yahya, A.O., Alaba, P.A., Aziz, A.R.A., Daud, W.M.A.W., 2015. Palm frond and spikelet as environmentally benign alternative solid acid catalysts for biodiesel production. BioResource. 10 (2), 3393–3408.
Sarpal, A.S., Costa, I.C.R., Teixeira, C.M.L.L., Filocomo, D., Candido, R., Silva, P.R.M., Cuhna, V.S., Daroda, R.J., 2016. Investigation of biodiesel potential of biomasses of Microalgae *Chlorella*, *Spirulina* and *Tetraselmis* by NMR and GC-MS techniques. J. Biotechnol. Biomater. 6, 2–17.
Singh, A., Pal, A., Maji, S., 2017. Biodiesel production from microalgae oil through conventional and ultrasonic methods. Energ. Source Part A: Recovery, Utilization, and Environmental Effects. 39 (8), 806–810.
Sinha, S.K., Gupta, A., Bharalee, R., 2016. Production of biodiesel from freshwater microalgae and evaluation of fuel properties based on fatty acid methyl ester profile. Biofuels. 7 (1), 69–78.
Sudarsanam, P., Zhong, R., Van den Bosch, S., Coman, S.M., Parvulescu, V.I., Sels, B.F., 2018. Functionalised heterogeneous catalysts for sustainable biomass valorisation. Chem. Soc. Rev. 47 (22), 8349–8402.
Suganya, T., Gandhi, N.N., Renganathan, S., 2013. Production of algal biodiesel from marine macroalgae Enteromorpha compressa by two step process: optimization and kinetic study. Bioresour Technol. 128, 392–400.
Supraja, K.V., Behera, B., Paramasivan, B., 2019. Optimization of process variables on two-step microwave-assisted transesterification of waste cooking oil. Environ Sci Pollut Res. 1–12.
Uchimiya, M., Bannon, D.I., Wartelle, L.H., 2012. Retention of heavy metals by carboxyl functional groups of biochars in small arms range soil. J. Agr. Food Chem. 60 (7), 1798–1809.
Wang, B., Gao, B., Fang, J., 2017. Recent advances in engineered biochar productions and applications. Crit. Rev. Env. Sci. Tec. 47 (22), 2158–2207.
Wang, S., Zhao, C., Shan, R., Wang, Y., Yuan, H., 2017. A novel peat biochar supported catalyst for the transesterification reaction. Energy Convers. Manag. 139, 89–96.
Yuan, T., Tahmasebi, A., Yu, J., 2015. Comparative study on pyrolysis of lignocellulosic and algal biomass using a thermogravimetric and a fixed-bed reactor. Bioresour Technol. 175, 333–341.
Zeng, D., Liu, S., Gong, W., Wang, G., Qiu, J., Chen, H., 2014. Synthesis, characterization and acid catalysis of solid acid from peanut shell. Appl Catal A Gen. 469, 284–289.
Zhang, J., Liu, J., Liu, R., 2015. Effects of pyrolysis temperature and heating time on biochar obtained from the pyrolysis of straw and lignosulfonate. Bioresour Technol. 176, 288–291.
Zhao, S.X., Ta, N., Wang, X.D., 2017. Effect of temperature on the structural and physicochemical properties of biochar with apple tree branches as feedstock material. Energies. 10 (9), 1293.